TRANSPARENCY EXTENSION IN HAPTIC INTERFACES VIA ADAPTIVE DYNAMICS CANCELLATION

Samuel McJunkin
Department of Mechanical Engineering
and Material Science
Rice University
Houston, TX
smcj@rice.edu

John E. Speich
Department of Mechanical Engineering
Virginia Commonwealth University
Richmond, VA
jespeich@vcu.edu

Marcia K. O'Malley
Department of Mechanical Engineering
and Material Science
Rice University
Houston, TX
omalleym@rice.edu

ABSTRACT

Haptic interfaces are a class of robotic manipulators that display force feedback to enhance the realism of virtual environment displays. However, these manipulators often fail to effectively replicate the real world environment due to dynamic limitations of the manipulator itself. The ratio of the simulated to transmitted environment impedance is defined as the transparency transfer function (TTF), and can be used to quantify the effectiveness of a haptic device in displaying the simulated environment. The TTF is ideally equal to one for the bandwidth of human proprioception. In this work, a method is presented that increases TTF bandwidth via cancellation of dynamics with an adaptive model. This adaptive model is based on the kinematics and dynamics of a PHANToM haptic interface with assumed joint stiffness and damping added. The Lagrangian of the PHANToM is reformulated into a regressor matrix containing the state variables multiplied by a parameter vector. A least-squares approach is used to estimate the parameter vector by assuming that errors in force output are due to the manipulator dynamics. The parameter estimate is then used in the original model to provide a feed-forward cancellation of the manipulator dynamics. Software simulation using data from passive user interactions shows that the model cancellation technique improves bandwidth up to 35 Hz versus 7 Hz without compensation. Finally, this method has a distinct advantage when compared with other compensation methods for haptic interactions because it does not rely on linear assumptions near a particular operating point and will adapt to capture unmodeled features.

INTRODUCTION

Haptic interfaces are a class of robotic manipulators that display tactile information from virtual or remote environments. When coupled with a visual and/or auditory display as in Figure 1, these manipulators enhance the realism of a virtual environment by immersing more of a user's sensory feedback mechanisms into the overall simulation experience.
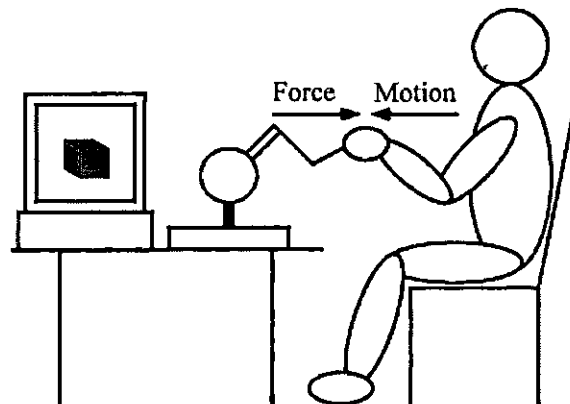

Figure 1 - Haptic interaction with graphic display

The environments that can be displayed are only limited by the imagination of the programmer and the limitations of the manipulator. These simulations can be used to deliver rehabilitation therapy to patients suffering the effects of a stroke, paralysis, or brain trauma [1]. Training is also possible as in the case of surgical procedures. Plus, these manipulators provide an alternative means of interpreting or displaying data. In short, haptic interfaces offer the promise of extending the usefulness of computers by allowing for a physical means of interaction.

Haptic Interactions

Generally, haptic interactions can be divided into two classes: active-user interactions (AUI) and passive user interactions (PUI). In an AUI, the user provides the motion input to the system and the response of the virtual environment is displayed through the manipulator; in a PUI, the manipulator plays a force through the manipulator while the user merely holds onto the manipulator. Both interaction types can be represented by the equations of motion for the system to be displayed; this can be expressed generally as in Equation 1

$$f(x,t) = g[x(t)] \qquad (1)$$

where f is the force output of the desired environment, and g is the function defining that environment as a function of time, t, and space, x. These types of interactions are displayed on impedance-based manipulators; so named because this manipulator measures the velocity as the state input and force is the system output. AUI's are a subset of this general interaction; Figure 2 shows the block diagram of this interaction. Here, X_H is the measured velocity input, Z_E is the environmental impedance, F_D is the desired force, G_T is the transparency transfer function and F_M is the measured force transmitted to the user. The human is assumed to be a velocity source, and the environment is assumed to passive. PUI's are the more general of the two interactions since a PUI doesn't require that the environment be passive. Figure 3 shows a block diagram of a PUI. Here, F_C is the commanded force and is not passive since it can contribute energy into the interaction. Y_H is the human-machine admittance, which means that the measured force is treated as an effort source and the human and the manipulator are modeled as passive elements.
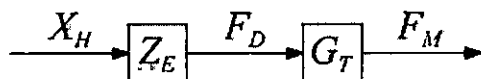

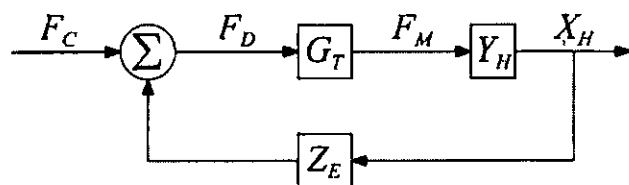Figure 2 - Block diagram of Active User Interaction (AUI)

Figure 3 - Block diagram of Passive User Interaction (PUI)

The commanded force, F_C, is usually a force playback meant to simulate a real interaction that cannot be displayed using AUI methods. This concept is known as event-based haptics because an event determines when the playback occurs. Examples of event-based haptics can be found in [2] and [3].

TRANSPARENCY AS A PERFORMANCE MEASURE

Transparency is defined as the ratio between transmitted and simulated impedance [4] where the ideal ratio is unity for desired bandwidth; this measure was originally used as performance measure in teleoperation systems, and will be discussed in detail in the next section. Other performance measures exist and rely on human perception or provide limit on displayable environments based on stability considerations. Transparency provides an intuitive measure of simulation fidelity, which can be used for feedback. A transparent haptic system enables a user to feel the virtual environment without sensation of manipulator dynamics. Moreover, the transparency bandwidth should be greater than the bandwidth of the displayed environment to ensure that high frequency content of the virtual environment is not attenuated when displayed to the human. Transparency measures how effectively a manipulator displays an environment; changes in transparency would reflect the need for compensators that adapt to those changes. In the case of virtual environments, transparency can be defined as the ratio of the measured force to the desired force, since the position of the manipulator endpoint and the human operator are coincident at the stylus of the device.

$$G_T = \frac{F_M}{F_D} \qquad (2)$$

For the purposes of this paper, bandwidth is defined as the $\pm 3dB$ crossover frequency from 0 dB for the transparency transfer function, which is the ratio defined above. The following sections describe the relevant literature for transparency as a performance measure in teleoperation and haptic systems. Then, a method used to improve performance in terms of transparency is presented.

Transparency in Teleoperation

Transparency and stability are of critical importance in teleoperation systems. The performance objectives of teleoperated systems are first to be stable and second to be transparent in the desired frequency range. Teleoperated systems face unique challenges related to communication lag, unknown human interaction forces, and the fact that the environment is not always well characterized. In short, a teleoperation system is generally a nonlinear, time varying system. Given that this is the case, attempts have been made with some success in [5-9] to characterize and control these unknowns to obtain stability and extend transparency bandwidth. Most attempts to date characterize the teleoperation system as a linear system. In such cases, the environment, human dynamics, and time lag are combined as disturbances and are linearized for analysis. As such, most of the techniques used to improve stability rely on compensators of some type

Linear compensators of the lead-lag type have been shown to extend transparency bandwidth [5, 6]. Other compensators use adaptive control laws to optimize for a given performance criteria, usually transparency or stability [7, 8]. In addition, it has been observed that unity transparency between the remote and the transmitted environment impedances is not always desirable [9]; Colgate observes that indeed it may be desirable to shape impedances to achieve stability and transmit impedances that are more meaningful to the user. Cases would include magnifying impedances in micro scale teleoperation or minimizing impedances in macro scale teleoperation.

Transparency in Virtual Environments

Transparency in virtual environments is merely a special case of teleoperation. In virtual environments, the goals are similar to that of teleoperation: maintain display stability and sufficient transparency bandwidth. In this work, transparency improvement is the primary objective, and stability will be treated in future work. Prior approaches to improve transparency and stability characteristics have been either with closed loop feedback [10] or open loop linear compensators [11], and implementation has been limited to simulation, Eom et al. have taken an approach to examine stability and transparency from a non-linear perspective where a disturbance observer is included in the haptic loop, and use Lyapunov stability criteria to verify stability [12]. This is a step closer to actually examining the general haptic interface, which is typically nonlinear in its kinematics, and therefore, dynamics. In this work, the authors improve upon previous methods by incorporating the nonlinear dynamics within a closed loop controller that will adaptively estimate the dynamics of the human and the manipulator.

PROBLEM DEFINITION

Previous data show that the transparency bandwidth for haptic devices does not extend beyond the bandwidth of human proprioception or tactile sensation [13]. As a result, simulations that attempt to display higher frequency information for higher fidelity cannot because human-manipulator dynamics become apparent at large velocities and accelerations. If these dynamics could be eliminated or counter-acted, the perceived dynamics would be due to the simulated environment alone. Therefore, the challenge is to develop a controller that makes this possible.

MANIPULATOR DYNAMICS

Figure 4 shows a block diagram of a PUI with the manipulator Lagrangian included and the proposed controller represented as feedback, $\tilde{\tau}_p$. Figure 4 is a block diagram of a PUI display with a coupling impedance, Z_E, and sufficiently illustrates that manipulator dynamics contribute to the overall displayed environment. Moreover, the manipulator transformation matrix, G_M, is merely the inverse of the Jacobian, which is never explicitly calculated as it represents the physical transformation of torques to forces via the manipulator mechanism. If torques due to the manipulator's dynamics can be estimated, it is possible to cancel the manipulator's dynamics.
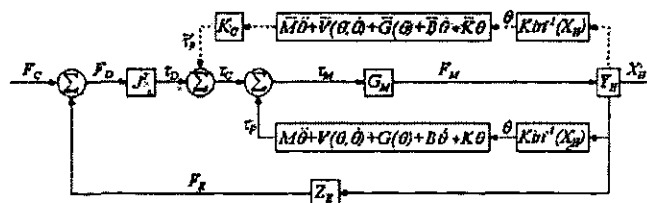
Figure 4 - Block diagram of a passive user interaction with manipulator dynamics included

The terms are defined as:

θ – desired joint-space trajectory
X_H – human trajectory
Z_E – environmental impedance
Y_H – human admittance
M – manipulator inertia matrix
V – manipulator Coriolis and centrifugal force vector
G – manipulator gravity force vector
B – joint dissipation matrix
K – joint stiffness matrix
F_C – command force
F_D – desired force
F_M – measured force
F_E – environment force
τ_D – desired torque
τ_C – command torque
τ_M – measured torque
τ_P – manipulator torque
$Kin^{-1}(\theta)$ – inverse kinematics
J^T – manipulator Jacobian
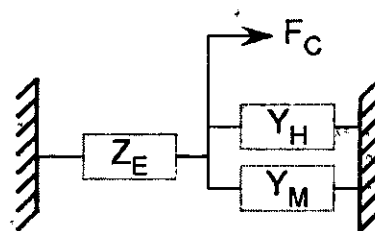G_M – manipulator transformation matrix
K_C – controller gain matrix

Figure 5 - Free-body diagram of passive user interaction, where Z_E is environment impedance, Y_H and Y_M are the human and machine admittances, and F_C is the commanded force

In the more general case of the PUI, the manipulator Lagrangian term can also include the human dynamics, Y_H, because the human and the manipulator, Y_M, are both grounded and are parallel to one another as in Figure 5. Therefore, it is assumed that the manipulator Lagrangian contains the human dynamics. This assumption requires that either the human be a linear time invariant (LTI) system or that the controller cancel these dynamics to adapt to changing dynamics due to the human.

CONTROLLER DESIGN

One way of correcting the force error due to unknown human-manipulator dynamics is to develop a means of estimating those dynamics as a function of the force output error and then use that estimate to correct the commanded torque to the manipulator.

First, define the desired end-point force, f_D, as

$$f_D = f(\ddot{x}_H, \dot{x}_H, x_H, t) \qquad (3)$$

where x_H represents the human motion input. The force due to manipulator dynamics, f_P, is defined as the difference between the desired force and the measured force, f_M,

$$f_P = f_D - f_M. \qquad (4)$$

By multiplying the manipulator dynamics by the Jacobian, it is possible to formulate the equations of motion in terms of the generalized coordintes where

$$J^T f_P = \tau_P \qquad (5)$$

and τ_P is the torque due to the manipulator. The Lagrangian derived by Cavusoglu et al [14], which defines the PHANToM 1.5A manipulator dynamics is

$$\tau_P = M\ddot{\theta} + V(\dot{\theta}, \theta) + B\dot{\theta} + K\theta + G(\theta). \qquad (6)$$

The matrices defining the compliant, K, and dissipative, B, dynamics are assumed to be symmetric, positive definite, passive, and decoupled because they occur at the joint. The inertial and gravitational forces and forces due to Coriolis and centrifugal forces are usually non-linear. In addition, the manipulator in this study is a PHANToM 1.0 Premium, but the Lagrangian derived by Cavusoglu et al provides the correct form since the differences between the two manipulators are scalars of manipulator parameters including: masses, moments of inertia, and link lengths.

To define the parameter update law, let us begin by defining an alternative form of the Lagrangian for convenience. The vector of torques due to the dynamics of the manipulator is a function of the displacement vector, its derivatives, and inertial, dissipative, and compliant elements. We can define this torque vector as a regressor matrix and coefficient vector

$$\tau_P = Y(\ddot{\theta}, \dot{\theta}, \theta)\Psi \qquad (7)$$

$$\Psi^T = \begin{bmatrix} \psi_1 & \psi_2 & \cdots & \psi_r \end{bmatrix} \qquad (8)$$

where Y is an $n \times r$ matrix of known functions, and Ψ is an $r \times 1$ vector of coefficients of the manipulator dynamics. The parameter space is not unique and the dimension, r, of the space depends on the choice of coefficient composition. The dimension, n, depends on the number of actuated degrees of freedom of the manipulator. This formulation has the advantage that it provides the opportunity to reduce the dimensional size of the parameter space by identifying parameters in the Lagrangian that share common functions of the generalized coordinates. The formulation of the regressor and the parameter vector can be found in the appendix.

To estimate the parameter vector, Ψ, a least-squares method is utilized. The torque estimate can be written as

$$\tilde{\tau}_P = Y(\ddot{\theta}, \dot{\theta}, \theta)\tilde{\Psi}. \qquad (9)$$

It is then possible to create a cost function based on the torque error between the manipulator's actual torque and its estimate. In this case, a quadratic cost function is used

$$J(\tau_P) = \tfrac{1}{2}(\tau_P - \tilde{\tau}_P)^T(\tau_P - \tilde{\tau}_P). \qquad (10)$$

The necessary condition is that the derivative of the cost function with respect to Ψ be zero defined as

$$\frac{\partial J(\tau_P)}{\partial \tilde{\Psi}} = (Y^T Y \tilde{\Psi} - Y^T \tau_P)^T = 0. \qquad (11)$$

Then, the estimate of Ψ can be defined as

$$\tilde{\Psi} = Y^T(YY^T)^{-1}\tau_P \qquad (12)$$

where the right pseudoinverse is used because Y is generally an underdetermined system of equations. Using the parameter estimate, it is now possible to define the controller in terms of the commanded torque, τ_C, as

$$\tau_C = \tau_D + K_C Y \tilde{\Psi} \qquad (13)$$

where K_C is a diagonal, positive definite gain matrix and acts as a proportional controller.

SIMULATION AND RESULTS

To test this hypothesis, the adaptive controller was implemented via simulation in MATLAB (The MathWorks, Inc.) using data from actual haptic interactions. The interaction consisted of a force chirp with amplitude of 4 N and a linear ramp in frequency from 0-100 Hz over a period of 30 seconds. In addition, virtual springs with a stiffness of 50 N/m were implemented as a coupling impedance; the springs provided a means of constraining the operating manipulator during the interaction. Figure 6 shows the physical set-up of the experiment with an inset showing the physical interpretation of the virtual environment model. This particular interaction also has the advantage of examining a typical operating environment and demonstrates the controller's viability. Figure 7 shows the results of the proposed adaptive controller. The top plot is the transparency magnitude in dB; the bottom plot is transparency phase in degrees. The x-axis is frequency measured in Hz. The solid line is the actual transparency of the measured to desired force ratio; the dotted line is the
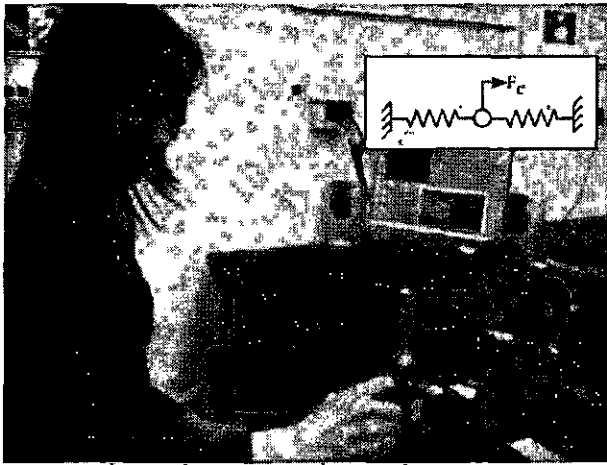
Figure 6 – Experimental set-up with model displayed at the endpoint

Figure 7 - Transparency transfer function estimates with and without the simulated controller

compensated transparency of the measured force to the desired force plus the compensated force. The simulation results in Figure 7 show that the controller does have an affect on transparency bandwidth. Crossover occurs at 7 Hz for the original PUI interaction and at 35 Hz after implementing the controller. The controlled system transparency shows a peak at 40 Hz contrasting with the notch in the original data. At 50 Hz, both the controlled system and the original data show a·roll-off at 50 Hz.

The bottom portion of the graph shows the phase of the TTF. The phase for the original data approaches -180 degrees between 50 and 60 Hz; the controlled system crosses 0 degrees between 10 and 30 Hz. The phase data indicates that the controller acts as a lead filter, but it is difficult to make a definitive statement since the controller is a non-linear controller while the magnitude-phase plot is a linear measure. Stability analysis can show that the augmented system is stable and will be addressed in future work.

The adaptive compensation method extends transparency bandwidth as well as other methods while being flexible to operating point changes because the model is capturing dynamics present in the system. It is known from Cavusoglu et al [14] that Phantom haptic interface system resonances occur between 50 and 100 Hz when measured for the X, Y, and Z axes independently. They suggest a forth-order model to capture the dynamics, which fits reasonably well to their experimental data. Therefore, it is not surprising that the data presented here closely match the data in the literature. These data also show that there may be bandwidth limitations of the amplifiers and motors of the Phantom, which are not addressed in this study. As a result, any proposed controller used to extend bandwidth will only be effective up to the bandwidth of the electromechanical hardware which explains attenuation at higher frequency.

DISCUSSION

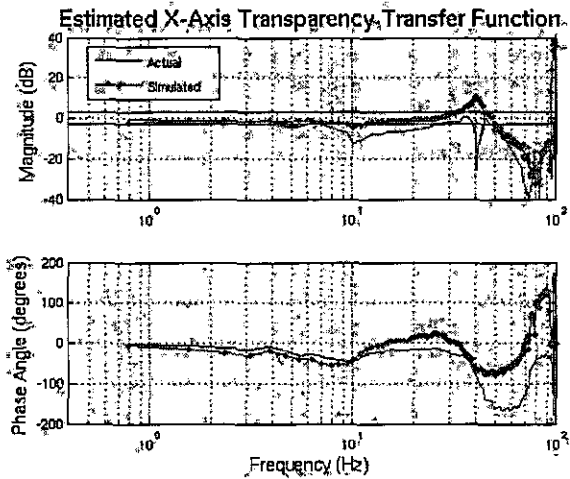The use of an adaptive model to eliminate human-manipulator dynamics improves transparency and performs, as well as, or slightly better than other controllers, and is a significant improvement over prior approaches because its nonlinear design is valid throughout the workspace and for a variety of users. Other control approaches such as linearized model cancellation or loop-shaping methods, discussed below, are designed for use near a particular operating point and do not adapt for different human users with varying dynamics of grip and posture. While the simulation results presented in this paper address an interaction only about a particular operating point in the device workspace (i.e. a linearized interaction), additional tests that examine a larger operation space with a variety of users will be necessary to validate the controller.

Other compensation methods have been used to extend transparency in certain applications, but are not sufficient for general compensation. These include open-loop methods such as lead-lag filters and other linear compensators, and closed-loop methods using the force error as the state-feedback variable. Open-loop linear methods do extend bandwidth because they cancel dynamics about a particular operating point. Kuchenbecker et al [15] demonstrated this in their work for displaying stiff surfaces using event-based haptics. Their display simulated the feel of virtual surface very well in comparison to a variety of displays; however, it did not adjust for the variety of users' postures. This is due to the fact that different users will have different stiffness, mass, and damping coefficients that comprise the assumed model. In addition, these linear compensators are generally only valid near the operating point where the data for the linear model was obtained. For comparison to the adaptive dynamics cancellation method, the authors implemented closed-loop force control for the Phantom device, but implementation proved infeasible due to difficulties in choosing appropriate controller gains. Force measurement as state feedback means that PD control is not feasible because of noise in the force derivative. PI control is offered as an alternative, but it too has problems because the integration term grows resulting in a steady-state error; PI force controllers are well suited for set-point force applications. However, haptic interactions are

1585

generally not set-point force applications; therefore, it makes sense to use a controller that estimates errors due to the system rather than simply using the error alone. Plus, it is difficult to choose controller gains based on a specific operating point that will maintain stability about an operating point that is constantly changing.

CONCLUSIONS

Transparency bandwidth extension is an important goal in haptic interactions because it provides a measure of whether the electromechanical system is actually displaying the forces as desired by the rendered environment. To this end, the method of canceling dynamics due to the human-machine interaction presented in this work makes it possible to have an adaptive model that increases transparency bandwidth. In addition, this method has advantages over traditional compensation methods because it does not rely on data from a particular operating point. Instead, it uses an a priori model and adapts the parameters to meet the desired performance criteria of transparency bandwidth extension.

ACKNOWLEDGMENTS

REFERENCES

1. M.K. O'Malley, (2005) "Shared control for upper extremity rehabilitation in virtual environments," Proceedings of the ASME International Mechanical Engineering Congress and Exposition DSC Division.
2. J.D. Hwang, M.D. Williams, and G. Neimeyer, (2004) "Toward Event-Based Haptics: Rendering Contact Using Open-Loop Force Pulses", 12th International Symposium on Haptic Interfaces for Virtual Environment and Teleoperator Systems, 24-31.
3. A.M. Okamura, R.J. Webster III, J.T. Nolin, K.W. Johnson, and H. Jafry, (2003) "The Haptic Scissors: Cutting in Virtual Environments", Proceedings of the IEEE 2003 International Conference on Robotics and Automation, 828-833.
4. D.A. Lawrence, (1993) "Stability and Transparency in Bilateral Teleoperation", IEEE Transactions on Robotics and Automation, pp. 9(5):624-637.
5. K.B. Fite, J.E. Speich, and M. Goldfarb, (2001) "Transparency and Stability Robustness in Two-Channel Bilateral Teleoperation", Journal of Dynamic Systems, Measurement, and Control, 123: 400-407.
6. J.E. Speich and M. Goldfarb, (2005) "An Implementation of Loop-Shaping Compensation for Multi-Degree-of-Freedom Macro-Micro Scaled Telemanipulation", IEEE Transactions on Control Systems Technology, 13(3): 459-464,.
7. H.K. Lee, and M.J. Chung, (1998) "Adaptive Controller of a Master-Slave System for Transparent Teleoperation", Journal of Robotic Systems,15(8):465-475.
8. K. Hashtrudi-Zaad and S.E. Salcudean, (2001) "Analysis of Control Architectures for Teleoperation Systems with Impedance/Admittance Master and Slave Manipulators", The International Journal of Robotic Research, 20(6):419-445.
9. J.E. Colgate, (1993) "Robust Impedance Shaping Telemanipulation", IEEE Transactions on Robotics and Automation, 9(4):374-384.
10. T. Sirithanapipat, (2002) "Haptic Interface Control Design for Performance and Stability Robustness", PhD Disseration, Vanderbilt University.
11. R.J. Adams and B. Hannaford, (2002) "Control Law Design for Haptic Interfaces to Virtual Reality", IEEE Transactions on Control Systems Technology, 10(1):3-13.
12. K.S. Eom, I.H. Suh, and B.J. Yi, (2000) "A Design Method of Haptic Interface Controller Considering Transparency and Robust Stability", Proceedings of the 2000 IEEE/RSJ Intl Conf on Robots and Systems (IROS) 961-966.
13. K. Shimoga, (1992) "Finger Force and Touch Feedback Issues in Dexterous Telemanipulation," in NASA-CIRSSE International Conference on Intelligent Robotic Systems for Space Exploration.
14. M. C. Cavusoglu, D. Feygin, and F. Tendick , (2002) "A Critical Study of the Mechanical and Electrical Properties of the PHANToM(TM) Haptic Interface and Improvements for High Performance Control.", Presence: Teleoperators and Virtual Environments, (11)6, 555-568.
15. K.J. Kuchenbecker, J. Fiene, G. Niemeyer, (2005) "Event-Based Haptics and Acceleration Matching: Portraying and Assessing the Realism of Contact", Proceedings of the 13th International Symposium on Haptic Interfaces for Virtual Environment and Teleoperator Systems and the First Joint World Haptics Conference, Pisa, Italy.

APPENDIX

Regressor Matrix, Y

$$Y = \begin{bmatrix} Y_A & Y_B & Y_C & Y_D & Y_E & Y_F \end{bmatrix}$$

$$Y_A = \begin{bmatrix} 0 & y_{12} & y_{13} \\ 0 & 0 & 0 \\ y_{31} & y_{32} & y_{33} \end{bmatrix}$$

$$Y_B = \begin{bmatrix} 0 & y_{15} & y_{16} \\ y_{24} & y_{25} & y_{26} \\ 0 & 0 & 0 \end{bmatrix}$$

$$Y_C = \begin{bmatrix} y_{17} & y_{18} & y_{19} \\ 0 & y_{28} & 0 \\ 0 & 0 & y_{39} \end{bmatrix}$$

$$Y_D = \begin{bmatrix} y_{110} & 0 & 0 \\ y_{210} & y_{211} & 0 \\ y_{310} & 0 & y_{312} \end{bmatrix}$$

$$Y_E = \begin{bmatrix} y_{113} & 0 & 0 \\ 0 & y_{214} & 0 \\ 0 & 0 & y_{315} \end{bmatrix}$$

$$Y_F = \begin{bmatrix} y_{116} & 0 & 0 \\ 0 & y_{217} & 0 \\ 0 & 0 & y_{318} \end{bmatrix}$$

$$y_{12} = (1 + \cos(2\theta_3))\ddot{\theta}_1 - 2\cos(\theta_3)\sin(\theta_3)\dot{\theta}_1\dot{\theta}_3 - \sin(2\theta_3)\dot{\theta}_1\dot{\theta}_3$$

$$y_{13} = (1 - \cos(2\theta_3))\ddot{\theta}_1 + 2\cos(\theta_3)\sin(\theta_3)\dot{\theta}_1\dot{\theta}_3 + \sin(2\theta_3)\dot{\theta}_1\dot{\theta}_3$$

$$y_{15} = (1 + \cos(2\theta_2))\ddot{\theta}_1 - 2\cos(\theta_2)\sin(\theta_2)\dot{\theta}_1\dot{\theta}_2 - \sin(2\theta_2)\dot{\theta}_1\dot{\theta}_2$$

$$y_{16} = (1 - \cos(2\theta_2))\ddot{\theta}_1 + 2\cos(\theta_2)\sin(\theta_2)\dot{\theta}_1\dot{\theta}_2 + \sin(2\theta_2)\dot{\theta}_1\dot{\theta}_2$$

$$y_{17} = \ddot{\theta}_1$$

$$y_{18} = (1 + \cos(2\theta_2))\ddot{\theta}_1 - 2\cos(\theta_2)\sin(\theta_2)\dot{\theta}_1\dot{\theta}_2 - \sin(2\theta_2)\dot{\theta}_1\dot{\theta}_2$$

$$y_{19} = (1 - \cos(2\theta_3))\ddot{\theta}_1 + 2\cos(\theta_3)\sin(\theta_3)\dot{\theta}_1\dot{\theta}_3 + \sin(2\theta_3)\dot{\theta}_1\dot{\theta}_3$$

$$y_{110} = 2\cos(\theta_2)\sin(\theta_3)\ddot{\theta}_1 - 2\sin(\theta_2)\sin(\theta_3)\dot{\theta}_1\dot{\theta}_2 + 2\cos(\theta_2)\cos(\theta_3)\dot{\theta}_1\dot{\theta}_3$$

$$y_{113} = \dot{\theta}_1$$

$$y_{116} = \theta_1$$

$$y_{24} = \ddot{\theta}_2$$

$$y_{25} = \sin(2\theta_2)\dot{\theta}_1^2$$

$$y_{26} = -\sin(2\theta_2)\dot{\theta}_1^2$$

$$y_{28} = 2\ddot{\theta}_2 + \sin(2\theta_2)\dot{\theta}_1^2$$

$$y_{210} = -\sin(\theta_2 - \theta_3)\ddot{\theta}_3 + \cos(\theta_2 - \theta_3)\dot{\theta}_3^2 + \sin(\theta_2)\sin(\theta_3)\dot{\theta}_1^2$$

$$y_{211} = \cos(\theta_2)$$

$$y_{214} = \dot{\theta}_2$$

$$y_{217} = \theta_2$$

$$\dot{y}_{31} = \ddot{\theta}_3$$

$$y_{32} = \sin(2\theta_3)\dot{\theta}_1^2$$

$$y_{33} = -\sin(2\theta_3)\dot{\theta}_1^2$$

$$y_{39} = 2\ddot{\theta}_3 - \sin(2\theta_3)\dot{\theta}_1^2$$

$$y_{310} = -\sin(\theta_2 - \theta_3)\ddot{\theta}_2 + \cos(\theta_2 - \theta_3)\dot{\theta}_2^2 - \cos(\theta_2)\cos(\theta_3)\dot{\theta}_1^2$$

$$y_{315} = \dot{\theta}_3$$

$$y_{318} = \theta_3$$

Parameter vector, Ψ

$$
\begin{bmatrix} \psi_1 \\ \psi_2 \\ \psi_3 \\ \psi_4 \\ \psi_5 \\ \psi_6 \\ \psi_7 \\ \psi_8 \\ \psi_9 \\ \psi_{10} \\ \psi_{11} \\ \psi_{12} \\ \psi_{13} \\ \psi_{14} \\ \psi_{15} \\ \psi_{16} \\ \psi_{17} \\ \psi_{18} \end{bmatrix}
=
\begin{bmatrix}
\left(I_{axx} + I_{dfxx}\right) \\
\frac{1}{2}\left(I_{ayy} + I_{dfyy}\right) \\
\frac{1}{2}\left(I_{azz} + I_{dfzz}\right) \\
\left(I_{bexx} + I_{cxx}\right) \\
\frac{1}{2}\left(I_{beyy} + I_{cyy}\right) \\
\frac{1}{2}\left(I_{bezz} + I_{czz}\right) \\
I_{baseyy} \\
\frac{1}{8}l_1^2\left(4m_a + m_c\right) \\
\frac{1}{8}\left(l_2^2 m_a + 4l_3^2 m_c\right) \\
\frac{1}{2}\left(l_1\left(l_2 m_a + 4l_3 m_c\right)\right) \\
\frac{1}{2}g\left(2l_1 m_a + 2l_5 m_{be} + l_1 m_c\right) \\
\frac{1}{2}g\left(l_2 m_a + 2l_3 m_c - 2l_6 m_{df}\right) \\
b_{11} \\
b_{22} \\
b_{33} \\
k_{11} \\
k_{22} \\
k_{33}
\end{bmatrix}
$$